



The effect of the geometry and content of the modified carbon nanotubes on the thermal properties of the composite phase-change materials

Min Li^{1,2} · Qiwen Chen¹ · Caiqian Yang³

Received: 5 March 2019 / Accepted: 8 December 2019 / Published online: 3 January 2020
© Akadémiai Kiadó, Budapest, Hungary 2020

Abstract

In this paper, ultrasonic dispersion and surface chemical modification were used to prepare the modified multi-walled carbon nanotubes (MWNTs)/paraffin composite phase-change materials (PCMs). The surface modification of MWNTs was developed via coating MWNTs with silica dioxide. The modified MWNTs were marked as SiO₂@MWNTs. The phase-change properties, thermal stability and chemical functional groups of the MWNTs/paraffin composite PCMs were measured by differential scanning calorimetry, thermogravimetric analysis (TG) and Fourier transform infrared spectroscopy, respectively. The results indicated that paraffin and MWNTs were compound physically. The diameter and content of MWNTs had influence on the phase-change temperature and the latent heat of the MWNTs/paraffin composite PCMs. The smaller the diameter or larger content of the SiO₂@MWNTs, the greater the influence was. The reduction degree of PCM1 (the diameter of the SiO₂@MWNTs is 20–30 nm) in latent heat is about 4.5 times of that of PCM3 (the diameter of the SiO₂@MWNTs is larger than 50 nm). The thermal stability and the thermal conductivity of the composite PCMs were improved with the addition of the SiO₂@MWNTs. When the content of SiO₂@MWNTs is 5 mass%, the thermal conductivity of the paraffin PCMs is 0.383 W m⁻¹ K⁻¹).

Keywords MWNTs · Modification · Thermal property · Phase-change materials

Introduction

Latent heat storage using phase-change materials is an effective method to improve energy efficiency and alleviate energy crisis. Organic PCMs are widely used in energy storage field due to having wide range of phase transition temperature, no phase separation and no super cooling degree [1] in the phase-change process. However, the low thermal conductivity of the organic PCMs restricts its heat transfer performance in practical applications. Mehdi

et al. investigated the effect of thermophysical properties of phase-change materials on melting process. The results revealed that using materials with lower specific heat and melting temperature caused the reduction in melting time [2]. The current research on improving the heat transfer mainly focuses on the addition of high thermal conductivity materials [3–8]. Masoud Jamalii's investigation showed that the rate of increase in heat transfer coefficient varies depending on diameter and type of nanoparticles [9]. Milad et al. [10] investigated the effects of adding copper and aluminum oxide nanoparticles to the paraffin. The results showed that the performance of heat sink was improved by adding a low percentage of nanoparticles (2%). However, by increasing volume fraction of nanoparticles to 6%, not only the heat sink performance did not improve, but also decreased. It can be seen that the content of nanoparticles affected the heat transfer of PCM remarkably.

CNT is one of the known materials with highest thermal conductivity. The thermal conductivity of the single-wall CNTs is about 6600 W m⁻¹ K⁻¹ [11], and the thermal conductivity of multi-walled CNTs is about 3000 W m⁻¹ K⁻¹

✉ Min Li
limin.li@163.com

¹ Jiangsu Key Laboratory for Construction Materials, Southeast University, Nanjing 211189, China

² Engineering Research Center of Building Equipment, Energy, and Environment, Ministry of Education, Nanjing 210096, China

³ College of Civil Engineering and Mechanics, Xiangtan University, Xiangtan 411100, China

[12]. This characteristic makes CNTs as a good heat conduction material and shows great potential for application in the field of heat transfer applications [13–15]. However, CNTs have large specific surface area and surface energy, which causes agglomeration of CNTs, thus affecting the thermal properties of the CNTs composite. Therefore, reducing the surface force and increasing the dispersion are the main problems to be solved in the preparation of CNTs composite PCMs. Islam et al. [16] adopted sodium dodecyl benzene sulfonate (SDBS) to modify SWNT, and the results showed that the modified CNTs with SDBS could significantly improve the dispersion property of CNTs in water. Luo et al. [17] used piranha solution to introduce carboxyl on the surface of the MWNT and then used the dicyandiamide and phenyl biguanide for acylation reaction. As a result, organic amino compounds were introduced successfully on the surface of the MWNT. The results showed that the modified MWNT with organic amino could significantly reduce the MWNT surface energy of dispersion and specific surface energy. The dispersity and interfacial bond strength of MWNT in epoxy resin were improved significantly. Hou et al. [18] adopted 4,4'-di(n-tetradecyl) diphenylmethane disulfate salt (DSDM) as the dispersant to disperse MWCNTs. The results showed that the modification by DSDM could make MWCNTs negatively charged, and the high surface potential indicated that a large quantity of DSDM molecules was absorbed on the MWCNTs surface, which accounted for the better dispersion property of the materials. Ma et al. [19] studied the dispersion of pristine and polyaniline-functionalized carbon nanotubes by Hansen solubility parameters (HSPs). The results showed that the location and boundaries of the MWCNT' HSPs changed after polyaniline functionalized. Oueiny et al. [20] studied the dispersing power of different phosphonic acid surfactants on MWCNT. The results showed that decylphosphonic acid (DPA) provided good dispersion stability.

The thermal conductivity of organic PCMs can be greatly improved by adding CNTs into the PCMs. Ji et al. [21] prepared cetylic acid/CNTs composite PCMs, and the results showed that the thermal conductivity of cetylic acid was enhanced significantly by adding CNTs. Li et al. [22] prepared stearic acid/multi-walled CNTs composite PCMs. The results showed that the thermal conductivity and the heat transfer of stearic acid were enhanced because of adding the carbon nanotubes. However, the natural convection of stearic acid in the liquid phase was weakened. Harish et al. [23] reported that single-wall CNTs increased the thermal conductivity enhancement of alkanes in the solid state and liquid state. When adding 0.25% single-wall CNTs, the thermal conductivity of the solid and liquid PCMs could be increased by 250% and 10%, respectively. The coefficient of thermal conductivity increased with the content of the single-wall CNTs. Myristic–stearic acids

eutectics/CNTs as composite PCMs were studied by Tang et al. [24]. The results indicated that with the addition of different mass fraction of the CNT (9%, 12% and 15%), the thermal conductivity of the composite PCMs was increased by 23.2%, 49.4% and 63.7% in solid state, and 15.6%, 32.0% and 39.7% in the liquid state. Dimberu et al. [25] investigated the thermal conductivity of N-doped carbon/myristic–stearic acids shape stable composite material. The N-doped carbon was adopted as the supporting material, and the largest loading mass of PCMs was up to 88%. The thermal conductivity was up to 117.65% higher than the pure PCMs. Li et al. [26] studied the thermal property of paraffin/porous TiO₂ foams. The carbon layer was employed to cover the TiO₂ foams for the thermal conductivity enhancement. The results showed that the adsorption quantity of paraffin in the paraffin/porous TiO₂ foams composite reached 62 vol% without leakage. With the covering of carbon layers, the thermal conductivity was increased from 0.303 to 1.059 W m⁻¹ K⁻¹.

Moreover, there were many studies using numerical simulation method to study the flow and heat transfer characteristics of nanofluids. Mir et al. [27] carried out a comprehensive study of two-phase flow and heat transfer of water/air nanofluid in an elliptical curved minichannel. The results indicated that the increase in volume fraction of nanoparticles leads to the enhancement of the temperature of central line of flow.

Although many studies have been conducted on the increasing of PCM thermal conductivity by adding nanoparticles, these studies focus the simple geometries and performances of PCM. The studies on the effect of CNTs on the other thermal performances of the composite PCMs such as the latent heat are very few. Although the present studies showed that the content of nanoparticles affected the heat transfer of PCM remarkably, the research on the influence of the diameter and content of carbon nanotubes on the phase-change characteristics of PCM is not enough. It is unknown whether the diameter of CNTs affects the phase-change temperature and the latent heat of the composite PCMs. The distribution state of nanoparticles and CNTs in the organic PCMs as well as the action between CNTs, and the organic PCMs should be improved in order to enhance the heat transfer effect. Therefore, the effect of the geometry and content of the modified carbon nanotubes on the thermal properties of the composite PCM was studied in this paper.

In this paper, the modified CNT/paraffin composite PCM coated with silica was prepared. Firstly, the CNTs were modified by silica coating, and then the composite PCMs were prepared by mixing the modified CNTs and paraffin. The phase-change temperature, latent heat, thermal conductivity and thermal stability of the CNTs/paraffin composite PCMs with different diameters and different contents were studied which has been not explored by

Table 1 The specifications of MWNTs

Samples	External diameter/nm	Length/ μm	Specific surface area/ $\text{m}^2 \text{g}^{-1}$
MWNTs-1	20–30	0.5–2	120
MWNTs-2	30–50	0.5–2	100
MWNTs-3	> 50	0.5–2	70

researchers. Results of the study will contribute the highly effective application of PCM.

Experimental

Materials

Paraffin, the melting point of which was 26–28 °C, was purchased from Rubitherm (Shijiazhuang) PCMS CO., LTD. Multi-walled carbon nanotubes (MWNTs) were obtained from Chengdu Institute of organic chemistry, Chinese Academy of Sciences. The specifications are shown in Table 1.

Modification of CNT

The first step was the acidification of CNTs. 2.5 g CNTs was weighed and put into a flask with three necks. Then, 400 mL mixed acid (Strong HNO_3 /concentrated $\text{H}_2\text{SO}_4 = 3:1$) was added into the ultrasonic water bath for dispersion for 1 h. The mixture was then stirred (1500 rpm) and refluxed for 10 h at 120 °C. After cooled to the room temperature, the mixture was washed by deionized water and then vacuum-filtered for 4–5 times. The reactant was put in 200 mL concentrated hydrochloric acid. Then, the mixture was stirred and refluxed for 12 h at 100 °C. The obtained reactant was washed by deionized water to vacuum-filtered for 4–5 times. The acidated CNTs (MWNTs–COOH) were obtained after being dried in vacuum drying oven at 80 °C for 12 h.

The second step is silica coating. 1 g MWNTs–COOH was mixed with 17 g anhydrous alcohol, 15 g deionized water, 2 g ammonia water in the flask with three necks. The mixture was stirred at high speed for 15 min. Then, 25 g tetraethoxysilane (TEOS) was poured into the mixture and the mixture was stirred for 12 h at 40 °C and then filtered. The obtained sample was put into N, N-two methyl (DMF) with ultrasonic dispersion for 15 min, and then, the mixture was filtered again. After 4–5 times of washing and filtration, the product was vacuum drying at 60 °C for 24 h, and the CNTs coated with silica (SiO_2 @MWNTs) was obtained.

Preparation of the SiO_2 @MWNTs/paraffin composite PCMs

100 g liquid paraffin was mixed with a certain amount of modified CNTs (SiO_2 @MWNTs) in the beaker. The mixture was stirred with magnetic stirring for 1 h and then dispersed for 3 h in a 50 °C ultrasonic water bath. After cooling to room temperature, SiO_2 @MWNTs/paraffin composite PCMs were obtained. The mix proportions of SiO_2 @MWNTs/paraffin composite PCMs with different diameters and contents are shown in Table 2.

Characterization

FTIR (Thermo Scientific Nicolet iS10, Thermo Electron Corporation, USA) was used to analyze the modified functional groups of MWNT. The dried samples were mixed with KBr and pressed into a pellet. FTIR spectra were recorded among the range of 400–4000 cm^{-1} .

The phase-change temperature, latent heat and specific heat of paraffin and its composite PCMs are tested by differential scanning calorimetry (DSC200F3Maia, Netzsch company, German). The samples in the Al crucible were scanned under N_2 atmosphere from –20 to 60 °C. The scanning rate was 5 °C min^{-1} .

The specific surface area and pore size analysis tester were used to test the specific surface area of the modified CNTs. Firstly, the sample was vacuum degassing for 3 h, and then the adsorption experiment was carried out at –195 °C.

Synchronous thermal analysis (STA 449 F3 Jupiter, Netzsch company, German) was used for thermal gravimetric analysis of composite PCMs based on CNTs. The heating rate was 5 °C min^{-1} in a nitrogen atmosphere (60 mL min^{-1}) from 50 to 400 °C.

Thermal conductivity of composite was measured using a Hot Disk Thermal Constant Analyzers (TPS2500, Hot Disk AB Company, Sweden). The probe is completely immersed in liquid composite PCMs based on CNTs in 30 °C, and the heating power is 30 mW.

Table 2 The mix proportions of SiO_2 @MWNTs/paraffin composite PCMs with different diameters and contents

Grouping	Paraffin/g	SiO_2 @MWNT/g	Diameter of SiO_2 @MWNTs/nm	SiO_2 @MWNTs percentage of paraffin/mass%
PCM	100	0	–	0
PCM1	100	3	20–30	3
PCM2	100	3	30–50	3
PCM3	100	3	> 50	3
PCM4	100	5	30–50	5
PCM5	100	10	30–50	10

Results and discussion

Analysis of specific surface area of the MWNTs

In order to observe the change of the specific surface area before and after MWNTs modification, the specific surface area of the samples was measured by a specific surface area and pore size analyzer. Multi-molecular layer adsorption theory, also known as BET theory, is the most widely used adsorption theory. Its formula is:

$$\frac{V^a}{V_m^a} = \frac{c(p/p^*)}{(1 - p/p^*)[1 + (c - 1)p/p^*]} \quad (1)$$

where V^a means the adsorption capacity under pressure P . V_m^a means the saturated amount of a monomolecular layer. p^* means the saturated vapor pressure of the adsorbed liquid. C means the adsorption constant. This formula can be written as a linear form:

$$\frac{p}{V^a(p^* - p)} = \frac{1}{V_m^a} + \frac{c - 1}{cV_m^a} \frac{p}{p^*} \quad (2)$$

A straight line was obtained by mapping $P/[V^a(p^* - p)]$ to p/p^* . According to the linear intercept b and slope k , V_m^a and c can be calculated. Putting V_m^a and c into Eq. 3, the specific surface area of adsorbent a_s can be obtained:

$$a_s = \frac{V_m^a}{V_0} L a_m \quad (3)$$

where V_0 means the volume of 1 mol gas in the standard state. L means the Avogadro constant. a_m means the cross-sectional area of a single adsorbed molecule.

The adsorption/desorption curves of modified MWNTs are shown in Fig. 1. As shown in Fig. 1, there is a slight difference between the three isothermal curves, but they all show the inverse S type. According to the BET isotherm classification method, the three curves belong to II type adsorption isotherms. The curve in the low pressure stage ($0 < P/P^* < 0.2$) rises slowly, showing the upward convex shape, which indicates that the adsorption layer transits from the single molecule layer to the multi-molecular layer. This upward convex shape is not obvious, which shows that the number of micro-pores in the sample is little. In the medium-pressure stage ($0.3 < P/P^* < 0.7$), the curve is slowly increasing, which shows that the pore distribution is uniform. However, in the high-pressure stage ($0.8 < P/P^* < 1.0$), the curve suddenly rises and the amount of adsorption increased significantly, which is mainly because of the fact that the pore structures formed by the accumulation of CNTs can generate the adsorption similar to large pores. It can be seen that the adsorption curves and desorption curves are not completely overlapped owing to a layer of nitrogen absorbed on the

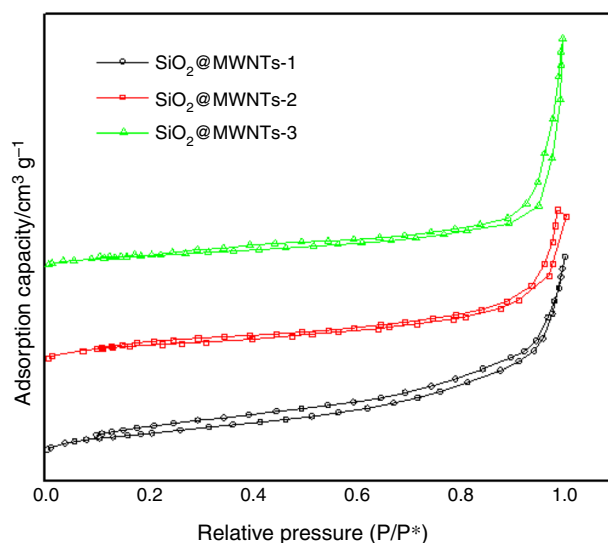


Fig. 1 The adsorption/desorption curves of MWNTs

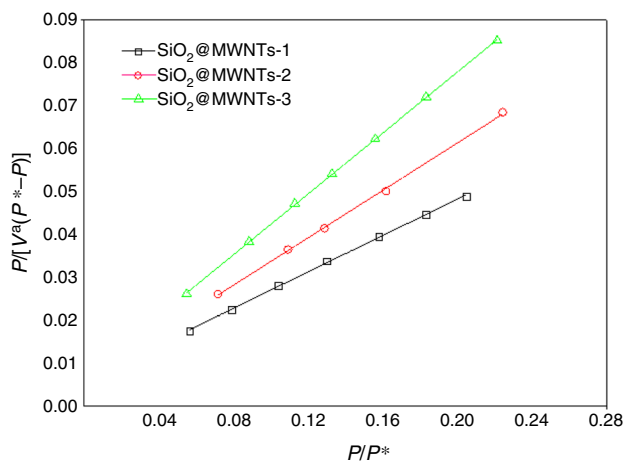


Fig. 2 Fitting straight lines of BET theory

pores on the hole wall. Therefore, under the same P/P^* , the desorption quantity is greater than that of the adsorption quantity.

The rectilinear of $P/[V^a(P^* - P)]$ and P/P^* of the three kinds of MWNTs is plotted and shown in Fig. 2. The intercept, slope and the calculation results of the specific surface area are listed in Table 3.

It is seen from Table 3 that the surface area of the modified MWNT is inversely proportional to the slope of the straight line, which can be derived from Eq. 3. The specific surface area of the modified MWNTs decreased significantly after being coated with silicon dioxide. The specific surface area of SiO_2 @MWNTs-1, SiO_2 @MWNTs-2 and SiO_2 @MWNTs-3 decreased by 83.4%, 84.6% and 82.8% separately. Table 3 indicates that the smaller the diameter of

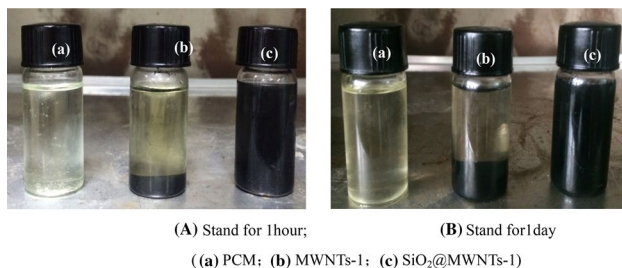
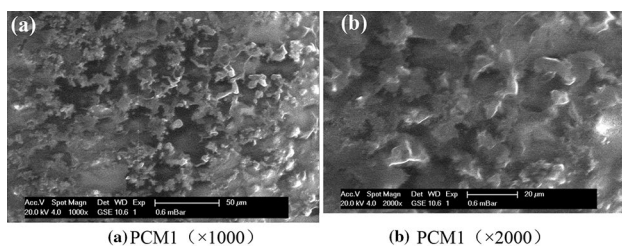
Table 3 The specific surface areas of the modified MWNTs

Specimen	<i>k</i>	<i>b</i>	$V_m^a/cm^3\ g^{-1}$	<i>c</i>	Specific surface area/ $m^2\ g^{-1}$
SiO ₂ @MWNTs-1	0.2123	0.0057	4.586	38.287	19.960
SiO ₂ @MWNTs-2	0.2769	0.0059	3.536	48.096	15.389
SiO ₂ @MWNTs-3	0.3552	0.0067	2.763	53.954	12.026

MWNTs before modification is, the larger the surface area of the SiO₂@MWNTs is.

The dispersion analysis

The MWNTs were mixed and stirred with paraffin by ultrasonic treatment for 2 h. Then, the mixture was introduced to a vacuum drying oven at 30 °C to prevent its solidification. The dispersion of MWNTs in paraffin is shown in Fig. 3. As shown in Fig. 3A, the MWNTs-1 before modification precipitated in paraffin after 1 h, while SiO₂@MWNTs-1 did not precipitate in paraffin. After 1d, the MWNTs-1 before modification had been completely precipitated in paraffin, while SiO₂@MWNTs-1 still dispersed well in paraffin, not appearing precipitation (Fig. 3B). It shows that the modified MWNTs coated with silica have good dispersion in paraffin

**Fig. 3** The dispersion of MWNTs in paraffin**Fig. 4** SEM micrographs of SiO₂@MWNTs-1/paraffin (PCM1)

wax. The reason is that after the modification, the specific surface area of the MWNTs-1 decreases and the surface force is reduced. Therefore, the aggregation is not inclined to occur. Moreover, the coating layer of SiO₂ has better intermolecular forces with the liquid paraffin molecules, which helps to increase the dispersion.

SEM analysis

SEM micrographs of SiO₂@MWNTs-1/paraffin (PCM1) under different magnification are shown in Fig. 4. It can be seen that the long white flocculent is SiO₂@MWNTs which was coated with paraffin. The length of the white flocculent is about several microns, which is consistent with that of the SiO₂@MWNTs. Figure 4 shows that the dispersion of SiO₂@MWNTs in the paraffin is relatively good, and no obvious agglomeration is found.

FTIR analysis

The Fourier transform infrared spectrograms of SiO₂@MWNTs/paraffin composite PCM are shown in Fig. 5. Paraffin is an alkane compound, which has obvious alkyl absorption peak at 2800–3000 cm⁻¹, 1460 cm⁻¹ and 1380 cm⁻¹. As shown in Fig. 5a, the peaks at 2682 cm⁻¹ and 2922 cm⁻¹ represent anti-symmetric stretch vibration of C–H in the CH₃ and CH₂ groups, respectively. The peak at 2850 cm⁻¹ is due to symmetric stretch vibration of C–H in the CH₂ group. The peak at 1462 cm⁻¹ is attributed to flexural vibration of C–H in the CH₃ and CH₂ groups. The peak at 721 cm⁻¹ represents vibration absorption peak of swaying bending of C–H in plane in the CH₂ group. The peak at 1379 cm⁻¹ is attributed to flexural vibration of C–H in the CH₃ group. The peak at 900 cm⁻¹ represents rocking flexural vibration of C–H out of plane in the CH₂ group.

The Fourier transform infrared spectrograms of SiO₂@MWNTs are shown in Fig. 5b, and the peak at 900 cm⁻¹ represents flexural vibration of C–H out of plane in carboxylic acid. The peak at 1100 cm⁻¹ is due to vibration of Si–O. The peaks at 1190 cm⁻¹ and 1640 cm⁻¹ represent stretch vibration of C–C and C=C in CNT wall graphite, respectively. The peak at 1379 cm⁻¹ is attributed to the flexural vibration of C–H for the CH₃ group, which is partly due to the incomplete hydrolysis of ethyl silicate.

Fourier transform infrared spectrograms of PCM1 are shown in Fig. 5c. It is consistent with the curve peak position of Figs. 5a, b two curves. Besides the corresponding peaks of Figs. 5a, b, there is no new peak appearing in Fig. 5c. This indicates no new material is formed after the compounding of CNTs and paraffin. That is to say, the compounding of CNTs and paraffin is merely a physical composite.

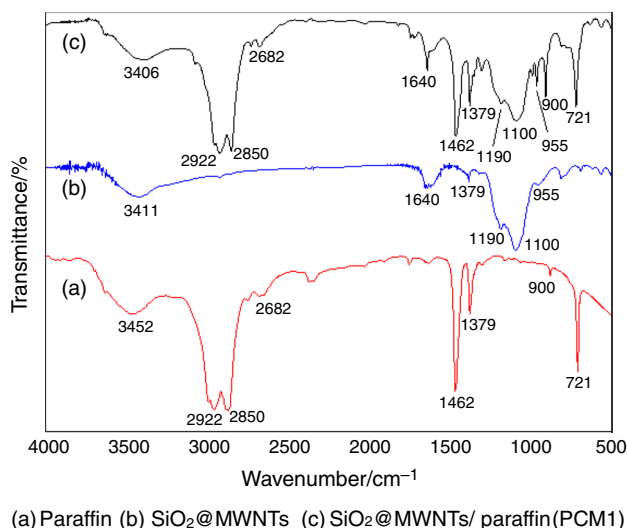


Fig. 5 Fourier transform infrared spectrograms of SiO₂@MWNTs/paraffin composite PCM

DSC analysis

1. The effect of the diameter of SiO₂@MWNTs on the phase transition properties of the composite PCMs

The DSC curves of the melting and solidification processes of the SiO₂@MWNTs/paraffin composite PCMs with different diameters of SiO₂@MWNTs are shown in Fig. 6. It can be seen that there are two-phase transition peak in the melting and solidification curves. The weaker peak is corresponded to the solid–solid phase transition of paraffin. The phase transition occurs in a wide temperature range, and the phase transition temperature of the melting process is higher than that of the solidification process, which results from the slight supercooling in the crystallization process [28].

The phase-change temperature (T_{om}), the phase transition temperature (T_{es}), the latent heat during melting (ΔH_m), the latent heat during solidification (ΔH_s) are listed in Table 4.

From Table 4, it can be seen that the phase transition temperatures of PCM1, PCM2 and PCM3 are lower than that of PCM. The addition of SiO₂@MWNTs reduces the phase transition temperature of paraffin, and the reduction degree varies inversely with the diameter of the SiO₂@MWNTs. The smaller the diameter of the SiO₂@MWNTs is, the lower the phase transition temperature of paraffin is. The reason is that the MWNTs have a certain effect on the binding force of paraffin molecules. The molecular arrangement of pure paraffin is regular, and the binding force is large, so it needs more energy to destroy the structure. After the SiO₂@CNTs is added into paraffin, the interaction between the SiO₂@MWNTs and the paraffin reduces the arrangement regularity of the paraffin molecules, and thus, the binding

force between the molecules of paraffin is decreased. As a result, the phase transition temperature is decreased. The smaller the diameter of SiO₂@MWNTs is, the greater its surface area and the surface energy are. This results in worse arrangement regularity of the paraffin molecules and weaker interaction between the paraffin molecules. Therefore, destroying the arrangement needs less energy. The phase transition temperature of paraffin is decreased consequently.

The latent heat of PCM1, PCM2 and PCM3 is less than that of PCM, and the smaller the diameter of the SiO₂@MWNTs, the more the latent heat decreases. Besides, the reduction degree of PCM1 in latent heat is about 4.5 times of that of PCM3. The reason is that the SiO₂@MWNTs with small diameter have large specific surface area and surface force, so it can absorb more paraffin molecules. The phase transition of paraffin is the transition from the order (disorder) to the disorder (order) actually. It is difficult for the absorbed paraffin molecules to take place this phase transition, so its latent heat is reduced.

2. The effect of the content of SiO₂@MWNTs on the phase transition properties of the composite PCMs

The DSC curves of melting and solidification processes of SiO₂@MWNTs/paraffin composite PCMs with different content of MWNTs are shown in Fig. 7. It can be seen that the latent heat and the phase transition temperature of the composites are ranked as: PCM > PCM2 > PCM4 > PCM5.

T_{om} , T_{pm} , T_{es} , T_{ps} , ΔH_m and ΔH_s of the SiO₂@MWNTs/paraffin composite PCMs are shown in Table 5.

Table 5 shows that the addition of SiO₂@MWNTs causes the decrease in the phase-change temperature and latent heat of the composite PCMs. From Table 5, it can be seen that the latent heat of the composite PCM decreases with the increase in the content of the SiO₂@MWNTs. The reason is that the addition of SiO₂@MWNTs causes the percentage content of paraffin in the composite to decrease. The latent heat of the composite PCM is provided by paraffin. In addition, the SiO₂@MWNTs with smaller diameter has large specific surface area and surface forces. When the SiO₂@MWNTs with higher content was compounded with paraffin, they can absorb more paraffin molecules. The adsorbed paraffin molecules are rearranged in the surface layer of the MWNTs, so the surface free energy of paraffin is affected. The surface free energy occupies a large proportion in the energy system of paraffin. According to the Second Law of Thermodynamics, the thermal properties of materials are influenced. Therefore, the more the content of SiO₂@MWNTs is, the smaller the latent heat of the composite PCMs is.

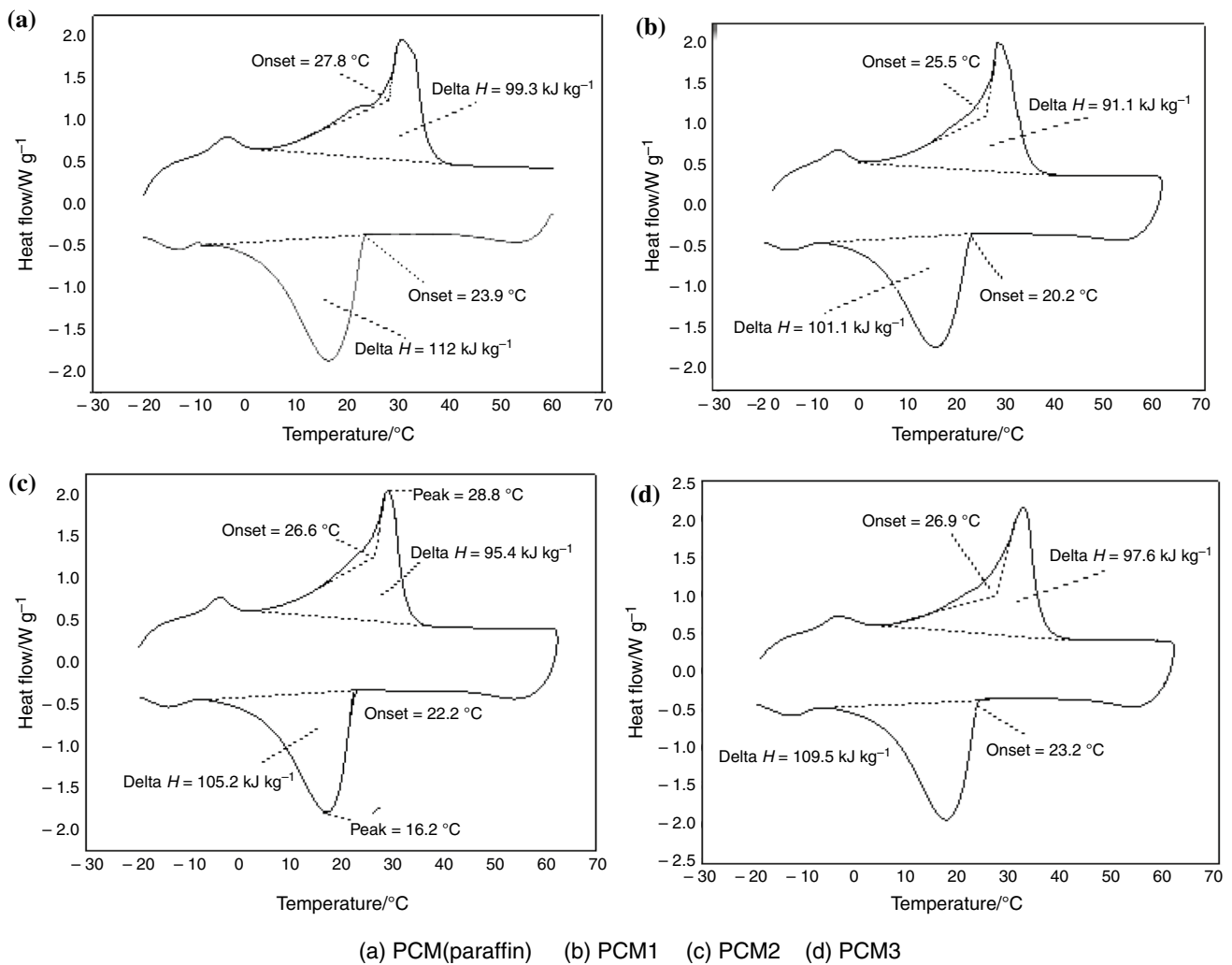


Fig. 6 DSC curves of the melting and solidification processes of the SiO₂@MWNTs/paraffin composite PCMs with different diameters of SiO₂@MWNTs

Table 4 The phase-change temperature and latent heat of SiO₂@MWNTs/paraffin composite PCM

Specimen	$T_{om}/^{\circ}\text{C}$	$\Delta H_m/\text{kJ kg}^{-1}$	$T_{es}/^{\circ}\text{C}$	$\Delta H_s/\text{kJ kg}^{-1}$
Paraffin	27.8	99.3	23.9	112
PCM1	25.5	91.1	20.2	101.1
PCM2	26.6	95.4	22.2	105.2
PCM3	26.9	97.6	23.2	109.5

Thermal stability analysis

TG curves of SiO₂@MWNTs/paraffin composite PCM under the atmosphere of nitrogen are shown in Fig. 8, which reflects the effect of the content of SiO₂@MWNTs on the thermal properties of the composites.

In the TG curves, the initial decomposition temperature of the composite phase-change material was considered as the

temperature of 5% mass loss. In this stage, water molecules and parts of paraffin waxes are gasified. When the content of SiO₂@MWNTs is 3%, 5% and 10%, the initial decomposition temperatures of PCM2, PCM4 and PCM5 are 123 °C, 145 °C and 164 °C, respectively, which shows that the initial decomposition temperature of paraffin increases with the addition of SiO₂@MWNTs ($T_{0.05}$ of paraffin is about 115 °C) [29]. The higher the content of SiO₂@MWNTs is, the higher the initial decomposition temperature is. The temperatures corresponding to total mass loss of paraffin in PCM2, PCM4 and PCM5 are 217 °C, 240 °C and 260 °C, respectively, which are all higher than that of pure paraffin (210 °C). In this stage, paraffin was completely gasified. The results showed that the temperature corresponding to total mass loss of paraffin in the composite PCMs increases with the increase in the content of SiO₂@MWNTs. Compared with paraffin, CNT has higher decomposition temperature that is 600–800 °C and better high-temperature resistance. Therefore, the addition of SiO₂@MWNTs helps to improve

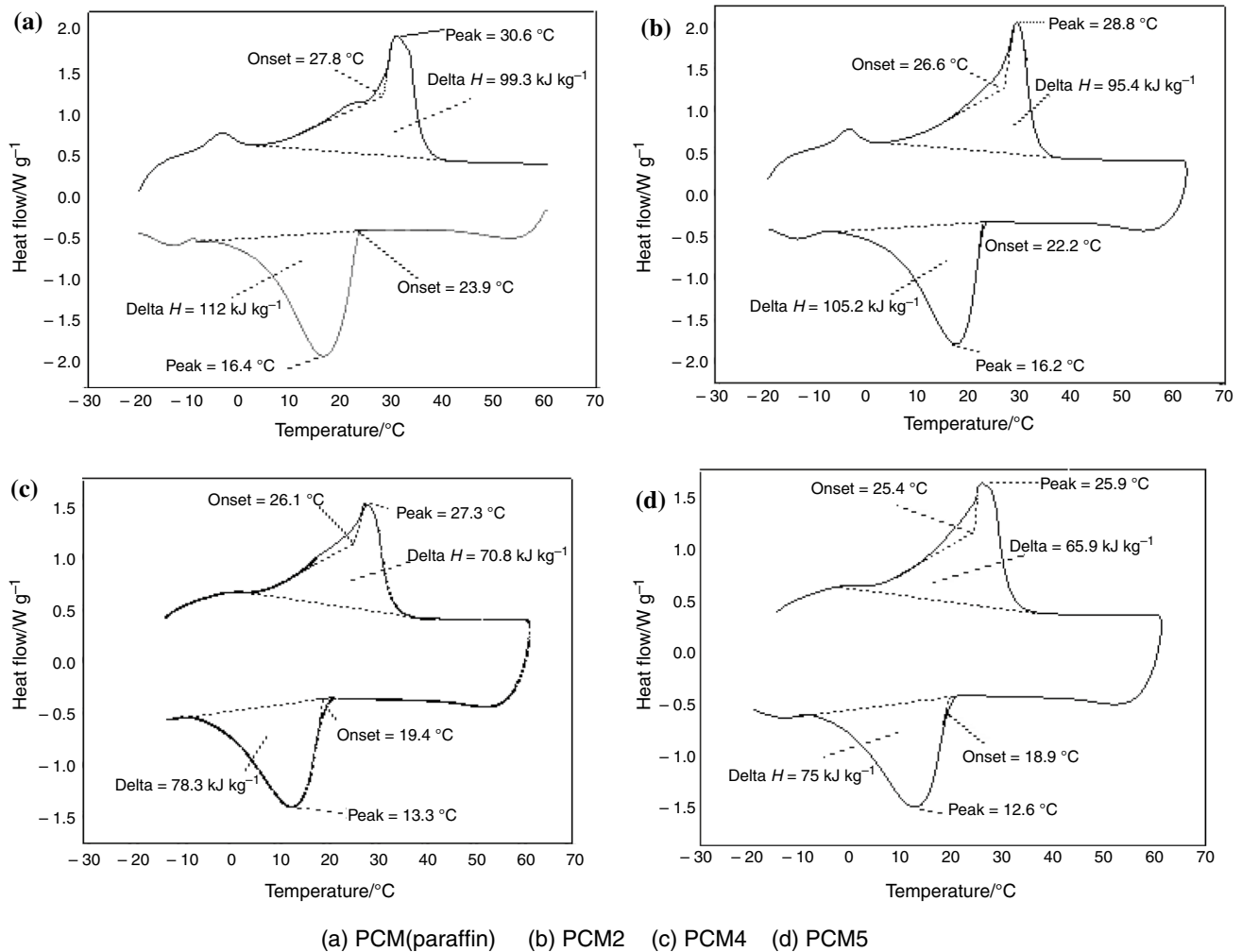


Fig. 7 DSC curves of the melting and solidification processes of SiO₂@MWNTs/paraffin composite PCMs with different content of MWNTs

Table 5 The phase-change temperature and latent heat of SiO₂@MWNTs/paraffin composite PCMs

Specimen	$T_{om}/^{\circ}\text{C}$	$T_{pm}/^{\circ}\text{C}$	$\Delta H_m/\text{kJ kg}^{-1}$	$T_{os}/^{\circ}\text{C}$	$T_{ps}/^{\circ}\text{C}$	$\Delta H_s/\text{kJ kg}^{-1}$
Paraffin	27.8	30.6	99.3	23.9	16.4	112
PCM2	26.6	28.8	95.4	22.2	16.2	105.2
PCM4	26.1	27.3	70.8	19.4	13.3	78.3
PCM5	25.4	25.9	65.9	18.9	12.6	75.0

the resistance of the composite. The higher the content of SiO₂@MWNTs is, the higher the thermal stability of the composite PCMs is.

Analysis on heat conductivity

The effect of SiO₂@MWNTs with different diameters on the thermal conductivity of paraffin PCMs is shown in Fig. 9. It can be seen that the thermal conductivity of paraffin is improved with the addition of MWNTs. In addition, the thermal conductivities of PCM1, PCM2 and PCM3 are more

than that of PCM. One reason is that paraffin can be attached to carbon nanotubes wall to nucleate, which belongs to the heterogeneous nucleation). Comparing to the homogeneous nucleation of the pure paraffin, the nucleation energy of paraffin on the surface of the SiO₂@MWNTs is smaller. This makes nucleation of paraffin on the surface of the SiO₂@MWNTs easier and accelerates the crystallization rate of paraffin. The other reason is that SiO₂@MWNTs is excellent heat transfer medium to promote nucleation and accelerate the crystallization rate.

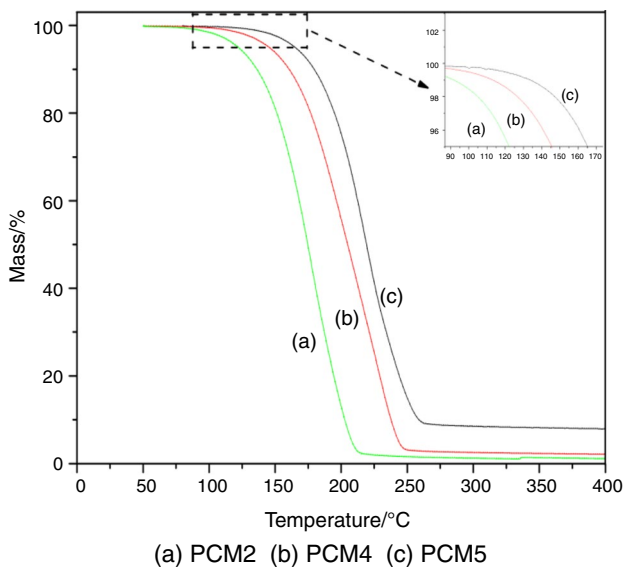


Fig. 8 TG curves of SiO₂@MWNTs/paraffin composite PCMs with different content of SiO₂@MWNTs

Figure 9 shows that when the content of SiO₂@MWNTs is the same, the smaller the diameter of carbon nanotubes is, the greater the thermal conductivity of paraffin PCMs is. Two reasons contribute to this result. The first one is that the interface thermal resistance exists between SiO₂@MWNTs and paraffin, which hinders the improvement of the thermal conductivity of the SiO₂@MWNTs on the paraffin matrix. So, reducing interfacial thermal resistance can improve the thermal conductivity. The other reason is, the smaller the diameter of CNT is, the larger its length to diameter ratio is. Consequently, the contact area between SiO₂@MWNTs and paraffin matrix is much greater, which is favorable for heat transfer.

The effect of SiO₂@MWNTs with different contents on the thermal conductivity of paraffin PCMs is shown in Fig. 10. It can be concluded from the figure that the thermal conductivity of SiO₂@MWNTs/paraffin composite PCM is gradually improved with the increase in the content of SiO₂@MWNTs. When the content of SiO₂@MWNTs is 5 mass%, the thermal conductivity of the paraffin PCMs is 0.383 W m⁻¹ K⁻¹. However, the thermal conductivity does not increase linearly with the increase in content SiO₂@MWNTs. The reason is that too much SiO₂@MWNTs will cause agglomeration and reduce the contact area between SiO₂@MWNTs and paraffin. As a result, the heat in the matrix cannot be transferred evenly and the heat transfer is limited to some extent.

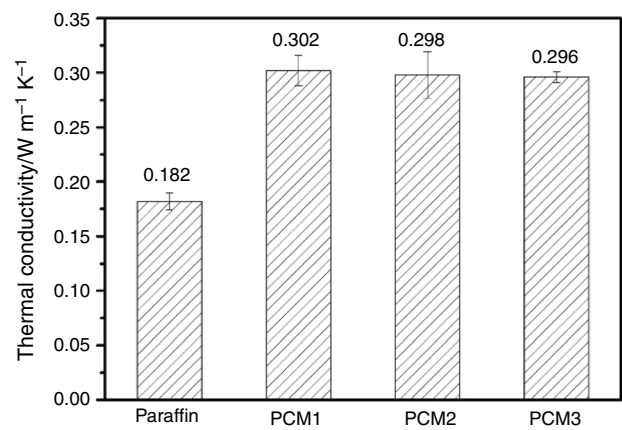


Fig. 9 Effect of SiO₂@MWNTs with different diameters on the thermal conductivity of paraffin PCMs

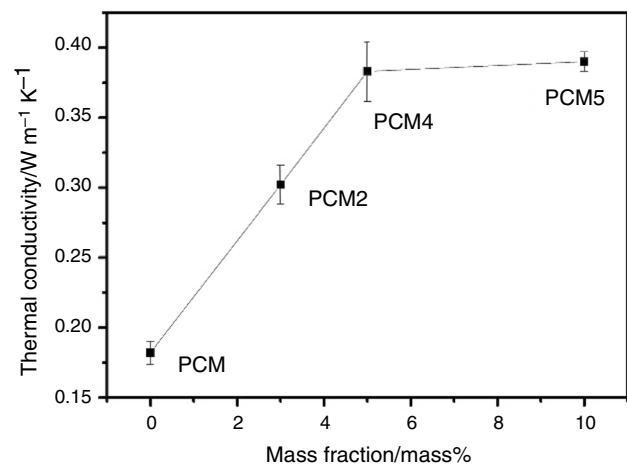


Fig. 10 Effect of different content of MWNTs on thermal conductivity of paraffin PCMs

Conclusions

The influence of the modified MWNTs on the thermal conductivity of the paraffin composite was investigated. Based on the study, the following conclusions can be drawn:

1. MWNTs are modified by being coated with silica. This modification method reduces the surface force and reduces the aggregation of MWNTs, which can improve the dispersion and thermal conductivity of paraffin.
2. The addition of the modified MWNTs makes the phase transition temperature and the latent heat of paraffin decrease correspondingly. In addition, the smaller the diameter of the SiO₂@MWNTs is, the smaller the latent heat and the phase transition temperature of the composite are. The latent heat and phase transition tempera-

ture decrease with the increase in the content of SiO₂@MWNTs.

3. The thermal conductivity of the composite PCM increases with the increase in the content of the SiO₂@MWNTs. The smaller the diameter of the MWNT is, the higher the thermal conductivity is.
4. After adding SiO₂@MWNTs, the temperature corresponding to the total mass loss of the paraffin in the composite PCM is improved, and it increases with the increase in the content of the MWNTs.

Acknowledgements This work was supported by the National Natural Science Foundation of China (51178102) which is financed by the National Natural Science Fund Committee. Financial support from Key R&D Program of Hunan Province (2018WK2111).

References

1. Berger C, Song Z, Li T, et al. Ultrathin epitaxial graphite: 2D electron gas properties and a route toward graphene-based nanoelectronics. *J Phys Chem B*. 2004;108(52):19912–6.
2. Miansari M, Nazari M, Toghraie D, et al. Investigating the thermal energy storage inside a double-wall tank utilizing phase-change materials (PCMs). *J Therm Anal Calorim*. 2019. <https://doi.org/10.1007/s10973-019-08573-2>.
3. Fan L, Khodadadi JM. Thermal conductivity enhancement of phase change materials for thermal energy storage: a review. *Renew Sustain Energy Rev*. 2011;15(1):24–46.
4. Fok S, Shen W, Tan F. Cooling of portable hand-held electronic devices using phase change materials in finned heat sinks. *Int J Therm Sci*. 2010;49(1):109–17.
5. Nurmawati MH, Siow KS, Rasiah IJ. Thermal performance of a phase change material on a nickel-plated surface. *Thin Solid Films*. 2004;462(1):481–6.
6. Martone A, Formicola C, Giordano M, et al. Reinforcement efficiency of multi-walled carbon nanotube/epoxy nano composites. *Compos Sci Technol*. 2010;70(7):1154–60.
7. Hou P, Mao J, et al. Improvement in thermodynamic characteristics of sodium acetate trihydrate composite phase change material with expanded graphite. *J Therm Anal Calorim*. 2019;137(4):1295–306.
8. Wei S, Duan Z, et al. Preparation and thermal performances of microencapsulated phase change materials with a nano-Al₂O₃-doped shell. *J Therm Anal Calorim*. 2019;138(1):233–41.
9. Jamali M, Toghraie D. Investigation of heat transfer characteristics in the developing and the developed flow of nanofluid inside a tube with different entrances in the transition regime. *J Therm Anal Calorim*. 2019. <https://doi.org/10.1007/s10973-019-08380-9>.
10. Bayat M, Faridzadeh MR, Toghraie D. Investigation of finned heat sink performance with nano enhanced phase change material (NePCM). *Therm Sci Eng Prog*. 2018;5:50–9.
11. Berber S, Kwon YK, Tomanek D. Unusually high thermal conductivity of carbon nanotubes. *Phys Rev Lett*. 2000;84(20):4613–6.
12. Kim P, Shi L, Majumdar A, et al. Thermal transport measurements of individual multiwalled nanotubes. *Phys Rev Lett*. 2001;87(21):215502–1–4.
13. Carlborg CF, Shiomi J, Maruyama S. Thermal boundary resistance among single-walled carbon nanotubes and surrounding matrices. *Phys Rev B*. 2008;78:205406–1–220546–8.
14. Gonnet P, Liang Z, Choi ES, et al. Thermal conductivity of magnetically aligned carbon nanotube buckypapers and nanocomposites. *Curr Appl Phys*. 2006;6:119–22.
15. Shaikh S, Lafdi K, Hallinan K. Carbon nanoadditives to enhance latent energy storage of phase change materials. *J Appl Phys*. 2008;103(9):094302–1–6.
16. Islam MF, Rojas E, Bergey DM, et al. High weight fraction surfactant solubilization of single-wall carbon nanotubes in water. *Nano Lett*. 2003;3(2):269–73.
17. Luo YF, Zhao Y, Cai JZ, et al. Effect of amino-functionalization on the interfacial adhesion of multi-walled carbon nanotubes/epoxy nanocomposites. *Mater Des*. 2012;33:405–12.
18. Hou J, Du W, Meng F, et al. Effective dispersion of multi-walled carbon nanotubes in aqueous solution using an ionic-gemini dispersant. *J Colloid Interface Sci*. 2017;512(15):750–7.
19. Ma J, Nan X, Liu J, et al. Dispersion of pristine and polyaniline functionalized carbon nanotubes in designed solvent mixtures by Hansen solubility parameters. *Mater Today Commun*. 2018;14:99–105.
20. Oueiny C, Berlioz S, Patout L, et al. Aqueous dispersion of multi-wall carbon nanotubes with phosphonic acid derivatives. *Colloids Surf A*. 2016;493:41–51.
21. Ji P, Sun H, Zhong Y, et al. Improvement of the thermal conductivity of a phase change material by the functionalized carbon nanotubes. *Chem Eng Sci*. 2011;81:140–5.
22. Li TX, Lee JK, Wang RZ, et al. Enhancement of heat transfer for thermal energy storage application using stearic acid nanocomposite with multi-walled carbon nanotubes. *Energy*. 2013;55:752–61.
23. Harish S, Ishikawa K, Chiashi S, et al. Anomalous thermal conduction characteristics of phase change composites with single-walled carbon nanotube inclusions. *J Phys Chem C*. 2013;117:15409–13.
24. Tang Y, Alva G, Huang X, et al. Thermal properties and morphologies of MA–SA eutectics/CNTs as composite PCMs in thermal energy storage. *Energy Build*. 2016;127:603–10.
25. Atinafu DG, Dong W, Huang X, et al. Introduction of organic–organic eutectic PCM in mesoporous N-doped carbons for enhanced thermal conductivity and energy storage capacity. *Appl Energy*. 2018;211:1203–15.
26. Li Y, Li J, Deng Y, et al. Preparation of paraffin/porous TiO₂ foams with enhanced thermal conductivity as PCM, by covering the TiO₂ surface with a carbon layer. *Appl Energy*. 2016;171:37–45.
27. Mir S, Akbari OA, Toghraie D, et al. A comprehensive study of two-phase flow and heat transfer of water/ag nanofluid in an elliptical curved minichannel. *Chin J Chem Eng*. 2019. <https://doi.org/10.1016/j.cjche.2019.07.007>.
28. Lecompte T, Le Bideau P, Glouanec P, et al. Mechanical and thermo-physical behaviour of concretes and mortars containing phase change material. *Energy Build*. 2015;94:52–60.
29. Quanguo Huang, Wenbing Yang, Kai Zhang. The preparation and characterization of polystyrene/paraffin phase change microcapsule. *Funct Mater*. 2014;45(13):13131–4.

Publisher's Note Springer Nature remains neutral with regard to jurisdictional claims in published maps and institutional affiliations.